Computation of SAR in Human Eye and Pregnant Woman Using Different Simulation Tools

Zlatko Živković, Duje Despalatović, Dragan Poljak, Antonio Šarolić, and Khalil El Khamlichi Drissi

Original scientific paper

Abstract: **Electromagnetic modeling of large scale problems arising from complex geometries, such as the human body or the specific organ, is generally undertaken by numerical methods implemented in simulation software packages. The structures involving high discretization density (mainly based on Magnetic Resonance Imaging and handled by Finite Difference Time Domain method) consume tremendously high computational cost. On the other hand, oversimplified numerical models may result in significantly less accuracy. The aim of this work was to investigate how detailed numerical model could be created using standard personal computer. Two rather complex cases of exposure were analyzed: human eye and pregnant woman exposed to radiofrequency electromagnetic radiation. The SAR distribution, peak localized 10g-averaged SAR and volume-averaged SAR in these models were determined using two software packages based on different numerical methods: FEKO software based on Finite Element Method and SEMCAD X software based on Finite Difference Time Domain method. The obtained results were compared to the results arising from other scientific studies which included the models of different complexity solved by different numerical methods.**

Index terms: **the human eye model, the pregnant woman model, SAR, FEKO, SEMCAD X, FEM, FDTD**

I. INTRODUCTION

The rapid growth of modern communication systems has caused the increase of public concern about possible adverse effects of EM radiation to human health. Therefore, the influence of EM radiation on human health has become very interesting research topic. The detailed description of the research that has been done so far is presented in [1]. As the human body presents electromagnetically complex structure, it is generally analyzed using numerical methods. Furthermore, as measurements of absorbed EM energy inside the human body are not possible, the phantoms with equivalent electrical parameters are often used [2-4].

The numerical models existing in literature can be divided in two groups regarding discretization density and tissues involved in the analysis. The realistic models of the human body (or organs) with a high discretization density are mainly based on Magnetic Resonance Imaging (MRI) [1], [5-10] and require enormous memory capacity same as high processor speed. On the contrary, more simplified models, with lower discretization density and lower demands on computer resources, [1-4] and [11], fail to ensure accurate results. Discretization density becomes particularly important at high frequencies so the simplified models can only be used to a certain extent.

In this paper 3D models of the human eye and pregnant woman were developed in order to estimate how a detailed numerical model can be analyzed using PC with a common nowadays configuration (4-6 GB RAM, 2 GHz processor). The simulations were carried out at standard GSM frequencies (900 and 1800 MHz), and additionally at 150 MHz for the pregnant woman model. Regarding the fact that the basic restriction according to ICNIRP [12], at these frequencies, is defined by Specific Absorption Rate (SAR), its distribution, peak localized 10g-averaged value and volume-averaged value in the examined models were calculated.

The human eye and pregnant woman model, respectively available in literature [1-11] and [13], are based on different numerical methods and include geometries of different complexity (realistic and simplified models) exposed to different radiation sources. The comparison of the results among these studies can be problematic and certain discrepancies could be expected. Therefore, in this study, the identical models of the human eye and the pregnant woman were developed using two software packages based on different numerical methods: FEKO [14] - based on Finite Element Method (FEM) and SEMCAD X [15] - based on Finite Difference Time Domain (FDTD) method. The computer requirements for each model and both numerical methods were estimated and the results for SAR distribution, peak localized 10g-averaged SAR and volume-averaged SAR (obtained using FEM and FDTD methods) were compared. The results were also compared with those available in relevant literature.

II. SIMULATION MODELS

A. The human eye model

The considered model of the human eye (without the head) is presented in Fig. 1a. The model consists of seven tissues: anterior chamber, cornea, ciliary muscle, lens, retina, sclera and vitreous humour. The electrical properties of the eye tissues at the specific frequency are available in [16] and [17] and are listed in Table 1 together with tissue density.

Manuscript received December 20, 2011; revised March 15, 2012.

This research was supported by the Ministry of Science, Education and Sports of the Republic of Croatia (Projects No. 023-0000000-3273, No. 023-0231582-1585 and No. 036-0361630-1631).

The material in this paper was presented in part at the 19th International Conference on Software, Telecommunications and Computer Networks (SoftCOM 2011), Split-Hvar-Dubrovnik, Croatia, Sept. 2011.

Z. Živković, D. Despalatović, D. Poljak and A. Šarolić are with the University of Split, Croatia (e-mail: {zlatko.zivkovic, dragan.poljak, antonio.sarolic}@fesb.hr, duje.despalatovic@gmail.com).

K. E. K. Drissi is with the Blaise Pascal University, France (e-mail: drissi@lasmea.univ-bpclermont.fr).

1845-6421/12/8247 © 2012 CCIS

The dimensions of the eye and its tissues are also available in literature [18]. The eye has been modelled using geometric bodies (cylinder, sphere, cone etc.) which then have been combined in unique model using standard Boolean operations.

For the purpose of FEKO/FEM analysis, the model has been meshed with about 60000 tetrahedra. Hence, the edge length of each tetrahedron has been set to 1 mm. This was found to be the upper mesh limit which could be solved with the dual core 32-bit PC equipped with 4 GB RAM. The detailed view of discretized structure is shown in Fig. 1b.

The same model for SEMCAD X/FDTD analysis has been voxeled with nearly 3 Mcells for the plane wave exposure and with nearly 4 Mcells for the dipole antennas exposure (which yielded the average voxel size in the eye of approximately 0.2×0.2×0.2 mm^3 for both types of radiation sources). Although even higher resolution could be run on such a computer (dual core 32-bit PC, 4 GB RAM), the computational cost would increase rapidly, without any significant improvement in the results accuracy. The voxeled representation of the model is shown in Fig. 1c.

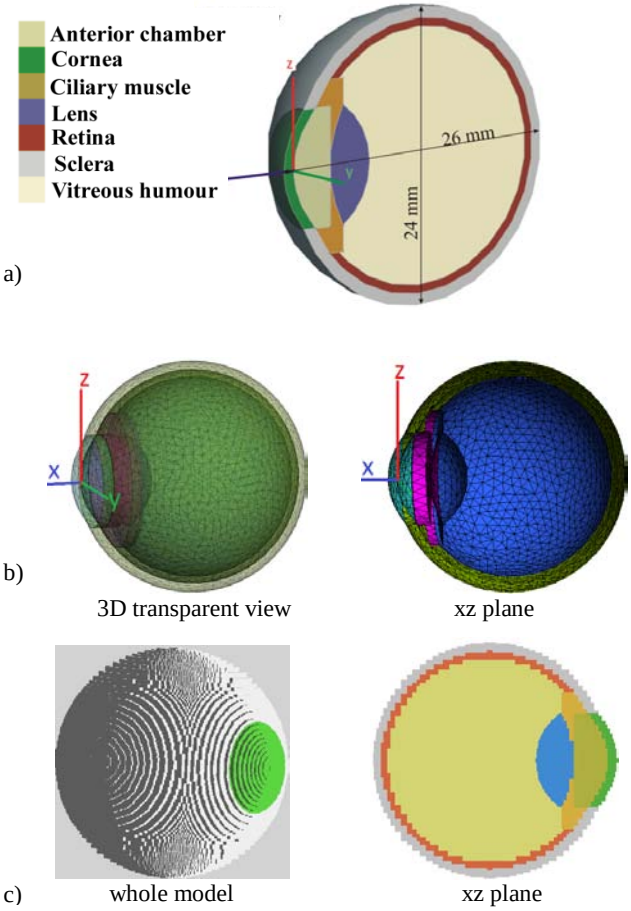

Fig. 1. a) Numerical model of the human eye, b) Meshed model (FEKO/FEM), c) Voxeled model (SEMCAD X/FDTD):

The eye model was exposed to two different sources of radiation – vertical short dipole (0.1λ long, divided in 20 wire segments for FEKO analysis) with radiated power P_{rad}=1 W which was placed at the distance d=10 cm in front of the eye (Fig. 2a) and vertically polarized incident plane wave with the power density S=5 mW/cm^2 (Fig. 2b). All simulations were performed at frequencies f=900 and f=1800 MHz, respectively.

TABLE I THE EYE TISSUE PROPERTIES

Tissue	f [MHz]	ε_r	σ [S/m]	ρ [kg/m^3]
Sclera	900	55	1.2	1170
	1800	53.9	1.5	
Retina	900	55.3	1.2	1039
	1800	53.5	1.6	
Cornea	900	55.2	1.4	1076
	1800	52.8	1.8	
Lens	900	46.6	0.8	1100
	1800	45.3	1.1	
Ciliary muscle	900	54.8	0.97	1040
	1800	53.8	1.22	
Anterior chamber	900	68.9	1.6	1010
	1800	68.6	2	
Vitreous humour	900	68.9	1.6	1000
	1800	68.6	2	

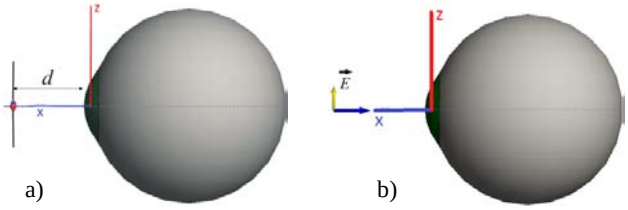

Fig. 2. Radiation sources: a) short dipole, b) plane wave

B. The pregnant woman model

The realistic model of the pregnant woman with all organs taken into account is too complex structure for analysis with standard PC equipment. Such a composite structure is therefore often replaced by a simplified model consisting of three parts: mother's torso, fetus and amniotic fluid [2-4] and [11]. The mother's torso was approximated with an elliptical cylinder while the fetus was replaced with an ellipsoid which was assumed to be immersed in the amniotic fluid. The electrical tissue properties of the fetus and the amniotic fluid were taken from [5], [11] and [17] and are listed in Table 2. The conductivity and permittivity of the mother's torso were calculated as 2/3 of the respective values for muscles given in [17], as suggested in [2], [3] and [19].

The detailed description of the analyzed model is shown in Fig. 3. The dimensions and geometrical properties of the model were taken from [4] for the comparison purposes.

The presented model required discretization to more than 150000 tetrahedra for FEM analysis with FEKO, which yielded the edge length of each tetrahedron of 1 cm. In spite of the mentioned geometric simplification, such a meshing

density was too dense to be carried out with PC equipped with 4 GB RAM. Hence, more powerful 64-bit PC with 6 GB RAM was used. The discretized structure is shown in Fig. 4, together with detailed preview of fetus and amniotic fluid discretization.

The pregnant woman model for SEMCAD X/FDTD analysis was voxeled in 4 Mcells for the plane wave exposure and in 4.5 Mcells for the dipole antennas exposure (which yielded the average voxel size in the pregnant woman model of approximately 3×3×3 mm^3 for both types of radiation sources). The calculation was carried out using the dual core 32-bit PC equipped with 4 GB RAM. The voxeled representation of the complete model and fetus immersed in the amniotic fluid is shown in Fig. 5.

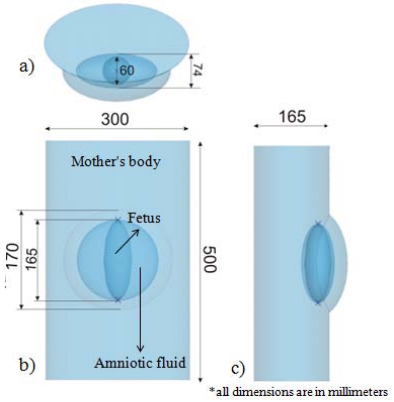

Fig. 3. Numerical model of pregnant woman: a) top view, b) front view, c) side view

TABLE II ELECTRICAL PARAMETERS OF A MOTHER'S TORSO, AMNIOTIC FLUID AND FETUS

Tissue	f [MHz]	ε_r	σ [S/m]	ρ [kg/m^3]
Mother's torso	150	42.1	0.50	907
	900	36.7	0.62	
	1800	35.7	0.90	
Amniotic fluid	150	78.3	1.23	986
	900	60.4	1.89	
	1800	76.0	2.15	
Fetus	150	76.9	0.91	967
	900	62.9	1.17	
	1800	60.4	1.89	

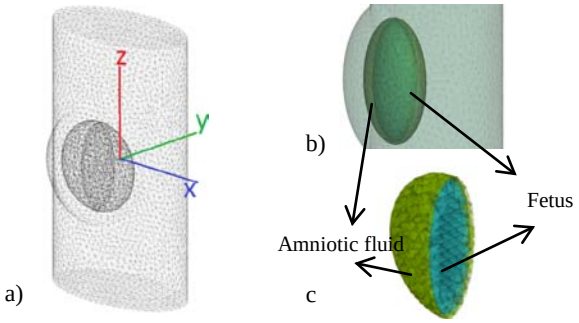

Fig. 4. Meshed model (FEKO): a) whole model, b) more detailed preview of mother's torso, c) fetus in amniotic fluid

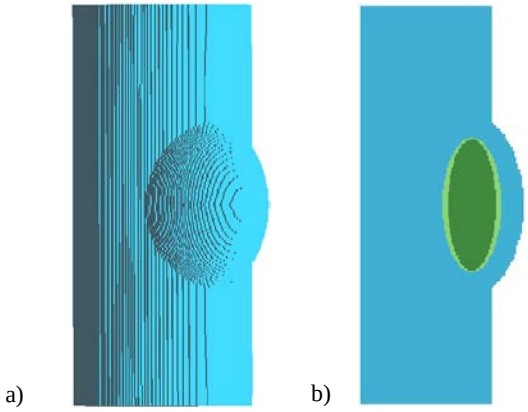

Fig. 5. Voxeled model (SEMCAD X): a) whole model, b) yz plane

The analyzed pregnant woman model was exposed to two different sources of radiation: dipole antenna (at 150, 900 and 1800 MHz), and the incident plane wave (at 900 and 1800 MHz). First, the vertical dipole (half-wave at 900 and 1800 MHz, 0.18λ long at 150 MHz, divided in 20 wire segments for FEKO analysis) with radiated power P_{rad}=1 W was placed at the distance d=6 cm in front of the torso (Fig. 6a). The model was analyzed for two different dipole positions: φ=0° and φ=-90° (Fig. 6a). Next, a vertically polarized incident plane wave with power density S=1 mW/cm^2 was used as the source (Fig. 6b). All parameters were chosen so the model could be compared with other scientific studies ([4-6] and [11]).

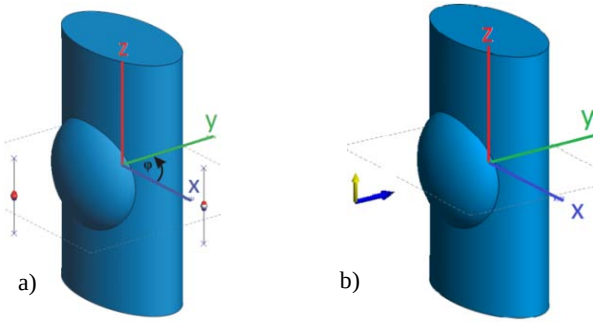

Fig. 6. – Radiation sources: a) dipole antenna, b) plane wave

III. SIMULATION RESULTS

A. SAR inside the human eye

SAR distribution simulation results for the human eye model are presented in Fig. 7 and 8 for FEKO/FEM analysis and in Fig. 9 and 10 for SEMCAD X/FDTD analysis. The results were obtained for *xy* and *xz* planes at frequencies f=900 MHz and f=1800 MHz for dipole antenna and plane wave radiation.

The obtained results clearly demonstrate that the position of the maximum induced SAR strongly depends on the frequency. At f=900 MHz the maximum SAR is induced in part of the eye closest to the radiation source (anterior chamber), while at f=1800 MHz the maximum SAR is induced in a deeper part of the eye (vitreous humour, right behind the lens).

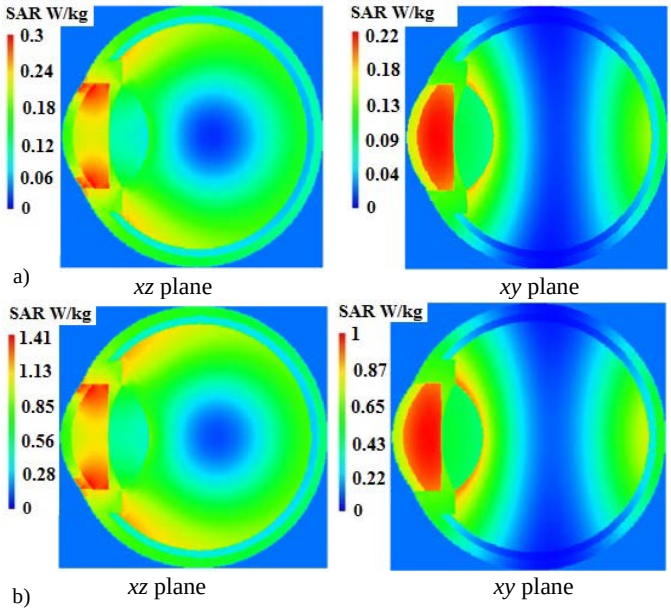

Fig. 7. SAR distribution at 900 MHz (FEKO):
a) dipole antenna exposure, b) plane wave exposure

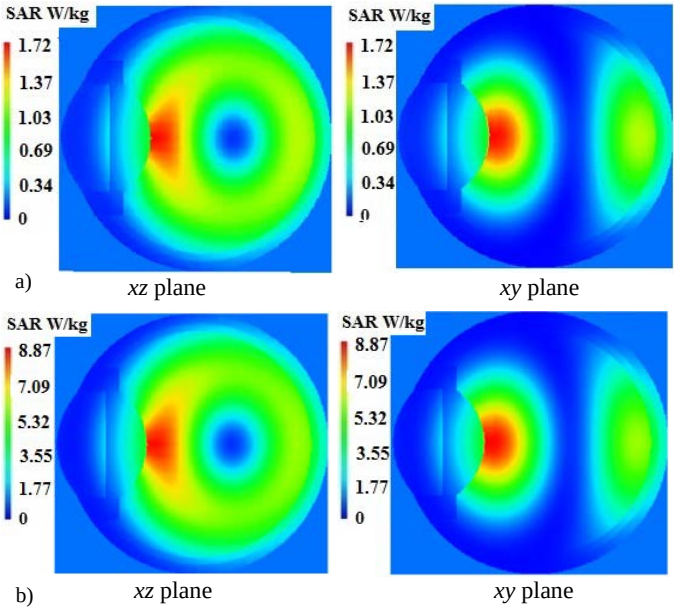

Fig. 8. SAR distribution at 1800 MHz (FEKO):
a) dipole antenna exposure, b) plane wave exposure

The similar results were obtained for the vertically polarized plane wave exposure at f=900 MHz in [16] and f=1800 MHz in [9], respectively. However, the maximum SAR in [16] is mainly induced in anterior chamber, while in [9] is mainly induced in vitreous humour, regardless the operating frequency. This difference could be explained by significant differences in developed eye models. In [16] 2D numerical model of human eye surrounded by head tissues was developed, based on MRI images. The SAR distribution in the eye was obtained by hybrid BEM/FEM method. In [9] an anatomically based 3D eye FDTD model involving the whole human head was developed. Although the realistic model of the human head was built, the simplified eye structure with only four tissues was modelled.

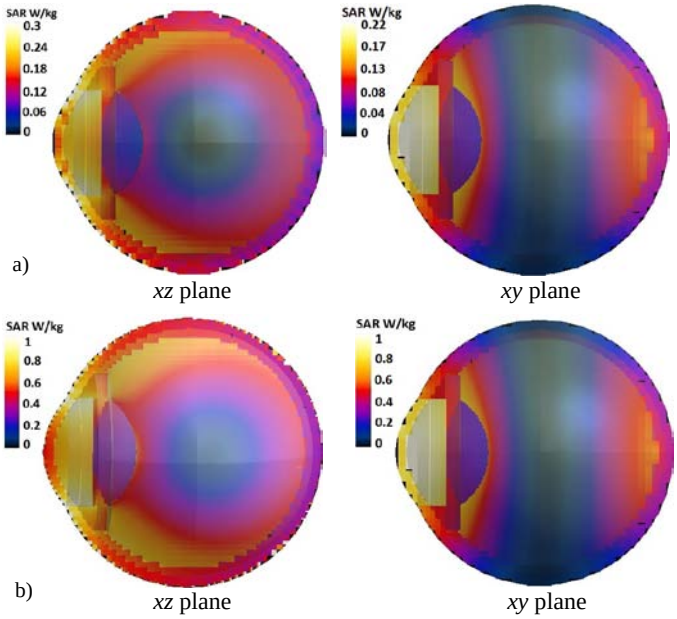

Fig. 9. SAR distribution at 900 MHz (SEMCAD X):
a) dipole antenna exposure, b) plane wave exposure

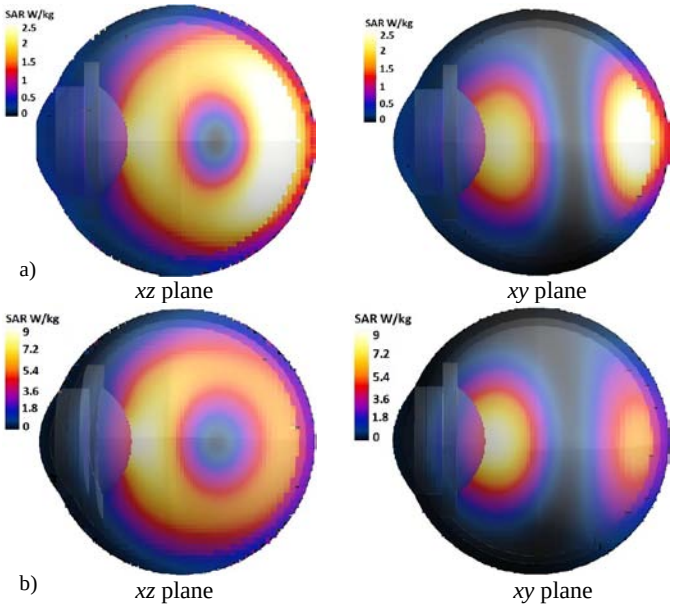

Fig. 10. SAR distribution at 1800 MHz (SEMCAD X):
a) dipole antenna exposure, b) plane wave exposure

The values of SAR averaged to whole eye are listed in Table 3. These values correspond also to 10g-averaged SAR, regarding the fact that the human eye weighs about 10 g [9]. The results were compared to ones available in [9] and [16] for plane wave exposure and to ones [8] for a dipole antenna exposure. The same dipole antenna model was used in this work for the purpose of comparison with [8]. Eye model in [8] is the same as in [9]. A very good agreement for f=1800 MHz could be noticed, while the results for f=900 MHz show more discrepancies. However, this is still in acceptable limits, when taking into account the model differences.

A rather satisfactory agreement of SAR distributions in the human eye, calculated using FEKO (Fig. 7 and 8) and

SEMCAD X (Fig. 9 and 10), can be observed. This is also the case for the whole eye averaged SAR results listed in Table 3.

TABLE III WHOLE EYE AVERAGED SAR – COMPARISON WITH LITERATURE

SAR [W/kg]	Antenna		Plane wave	
	900 MHz	1800 MHz	900 MHz	1800 MHz
FEKO/FEM	0.1	0.4	0.5	1.8
SEMCAD X/FDTD	0.1	0.4	0.4	2.1
H. Dodig [16] BEM-FEM	-	-	1.6	1.8
A. Hirata [9] FDTD	-	-	1.6	1.2
A. Hirata [8] FDTD	0.4	0.4	-	-

B. SAR in pregnant woman

SAR distribution simulation results at 900 and 1800 MHz for the pregnant woman model are presented in Fig. 11 and Fig. 12 for FEKO analysis and in Fig. 13 and Fig. 14 for SEMCAD X analysis. The results are presented for two different sources: dipole antenna positioned at φ=-90° (see Fig. 6a) and plane wave radiation. The maximum SAR values are induced in the part of mother's torso which is closest to the radiation source and in the amniotic fluid. However, in deeper parts of mother's body, SAR is progressively attenuated, ensuring negligible SAR values in fetus.

The values of peak localized 10g-averaged SAR and volume-averaged SAR are listed in Table 4.

The models given in [5-7] represent anatomically rather realistic model of the pregnant woman. The models were based on MRI images and analyzed with FDTD method. The vertically polarized plane wave with S=1mW/cm^2 at 900 MHz was used in [6]. The peak localized 10g-averaged SAR for the fetus was 0.01 W/kg, and for the mother's body 0.04 W/kg which represents a good agreement with values in Table 4, regarding significant model differences. The same plane-wave characteristics were used in [5]. The peak localized 10g-averaged SAR in fetus was 0.03 W/kg at 900 MHz and 0.02 W/kg at f=1800 MHz, which is still good accordance with our results.

TABLE IV PEAK LOCALIZED 10G-AVERAGED SAR AND VOLUME-AVERAGED SAR

	SAR [W/kg]	Dipole source				Plane-wave source			
		900 MHz		1800 MHz		900 MHz		1800 MHz	
		10g	avg	10g	avg	10g	avg	10g	avg
FEKO	Mother's body	1.25	0.01	1.12	0.006	0.3	0.05	0.22	0.05
	Amniotic fluid	0.62	0.07	0.26	0.03	0.09	0.05	0.02	0.05
	Fetus	0.24	0.11	0.12	0.03	0.06	0.02	0.03	0.02
SEMCAD X	Mother's body	1.25	0.01	1.09	0.007	0.3	0.06	0.23	0.04
	Amniotic fluid	0.62	0.10	0.27	0.03	0.16	0.05	0.08	0.04
	Fetus	0.25	0.10	0.12	0.03	0.08	0.02	0.04	0.01

The results for peak localized 10g-averaged SAR in fetus and the peak value of SAR in mother's body at 150 MHz, for different antenna positions (see Fig. 6a), are listed in Table 5. It is evident that the results, obtained with FEKO and SEMCAD X, are in a very good agreement with those reported in [4] and [11]. The more significant discrepancy only exists for the fetus with the antenna in position φ=0°. However, our model had larger amniotic fluid volume having resulted in more progressive electric field attenuation which caused lower SAR values in the fetus.

By comparing the simulation results obtained by FEKO/FEM and SEMCAD X/FDTD (Table 4 and 5, and Figures 11 to 14), a very good agreement can be observed for all frequencies and all radiation sources. However, the error was noticed in the results reported in [13], for the case of pregnant woman model exposed to the plane wave radiation. These results were obtained by specifying the effective value of the electric field instead of the electric field magnitude for the power density specification in FEKO simulation software (as indicated in FEKO manual [14]). Therefore, all erroneous results were corrected by scaling with factor 2.

TABLE V PEAK SAR AND PEAK LOCALIZED 10G-AVERAGED SAR AT 150 MHZ

SAR [W/kg]	φ=0°		φ=-90°	
	Fetus avg_10g	Mother's body Peak	Fetus avg_10g	Mother's body Peak
K. Ito [4] FDTD	-	-	0.36	1.15
H. Kawai [11] FDTD	0.1	1.3	-	-
FEKO FEM	0.03	1.6	0.34	1.4
SEMCAD X FDTD	0.03	1.5	0.36	1.3

It should be noted (from Table 4) that the volume-averaged SAR calculated for the fetus at 900 MHz (dipole source) is 0.11 W/kg (FEKO) and 0.10 W/kg (SEMCAD X). Both values exceed the limit of 0.08 W/kg given for whole-body average SAR by ICNIRP [12]. This raises the question regarding the limit applicable for the fetus exposure. The limits for localized 10g-averaged SAR given by ICNIRP (2 W/kg for head and trunk, 4 W/kg for limbs) are meant for body parts. However, fetus represents a whole body, possibly more sensitive to stress then the born human of any age. Fetus exposure, although considering as localized from mother's body, represents a whole-body thermal stress. Thus, the limit for whole-body average should be considered, and these results suggest the fetus might get overexposed.

IV. CONCLUSION

The SAR distribution, peak localized SAR and volume-averaged SAR inside the two anatomically complex geometries (human eye and pregnant woman) were analyzed with common nowadays office PC computer configurations, using FEKO software based on FEM method and SEMCAD X software based on FDTD method.

The human eye (without the head) with seven different tissues, discretized with about 60000 tetrahedra for

FEKO/FEM analysis, and with more than 3 Mcells for SEMCAD X/FDTD analysis, was successfully modelled and analyzed with a 32-bit 4 GB RAM personal computer. The realistic pregnant woman model was found to be too complex for analysis with such PC configuration, so the simplified geometrical model consisting just of mother's torso, amniotic fluid and fetus was developed. Even so, the model required discretization to more than 150000 tetrahedra for FEKO/FEM analysis. This model was too large to be solved with PC equipped with 4 GB RAM. Hence, more powerful 64-bit PC with 6 GB RAM had to be used.

The same model was discretized with more than 4 Mcells for the SEMCAD X/FDTD simulations and was successfully solved using a 32-bit 4 GB RAM personal computer.

All results obtained with SEMCAD X and FEKO were in a very good agreement. Moreover, the satisfactory agreement between these results and the results obtained with anatomically realistic FDTD models (based on MRI and available in relevant literature) was noticed.

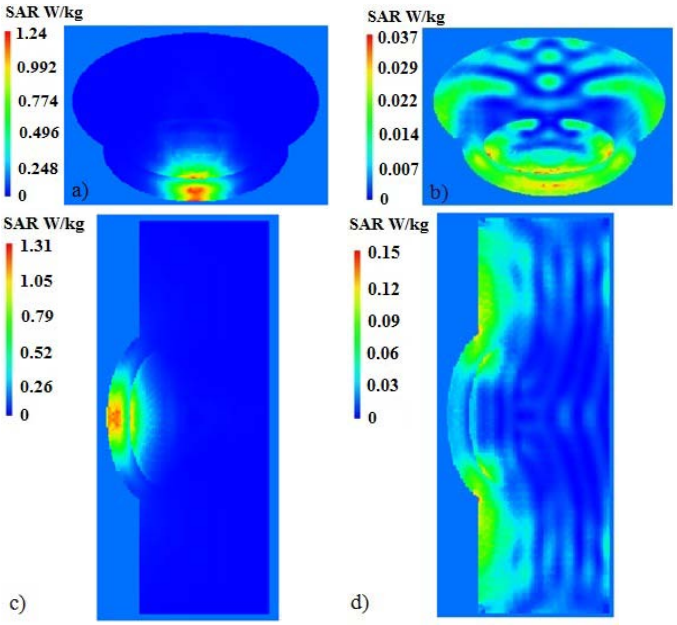

Fig. 11. SAR distribution at 900 MHz (FEKO):
a) xy plane, dipole source; b) xy plane, plane wave source;
c) yz plane, dipole source; d) yz plane, plane wave source

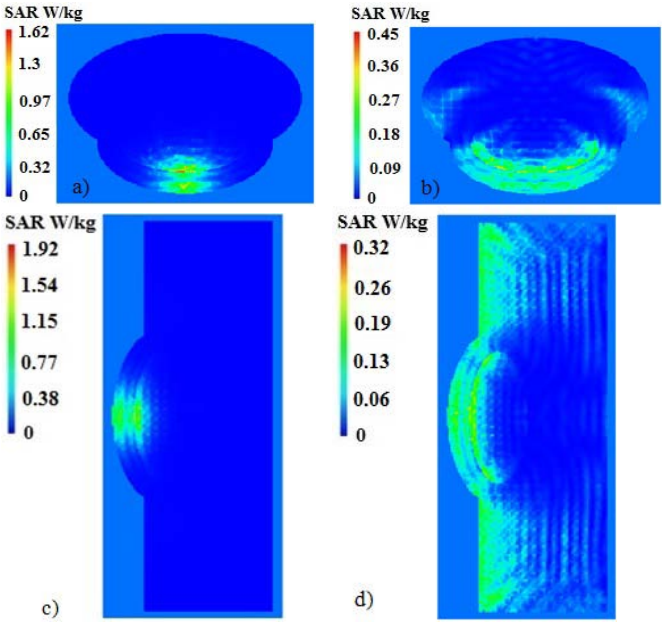

Fig. 12. SAR distribution at 1800 MHz (FEKO):
a) xy plane, dipole source; b) xy plane, plane wave source;
c) yz plane, dipole source; d) yz plane, plane wave source

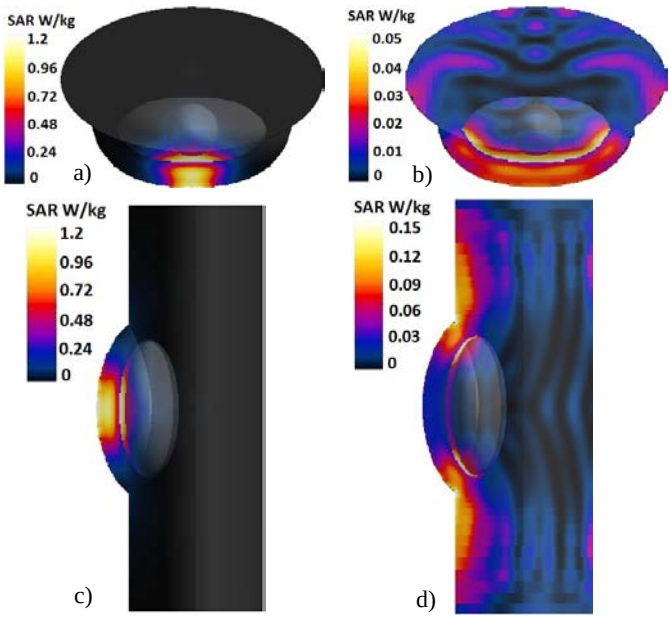

Fig. 13. SAR distribution at 900 MHz (SEMCAD X):
a) xy plane, dipole source; b) xy plane, plane wave source;
c) yz plane, dipole source; d) yz plane, plane wave source

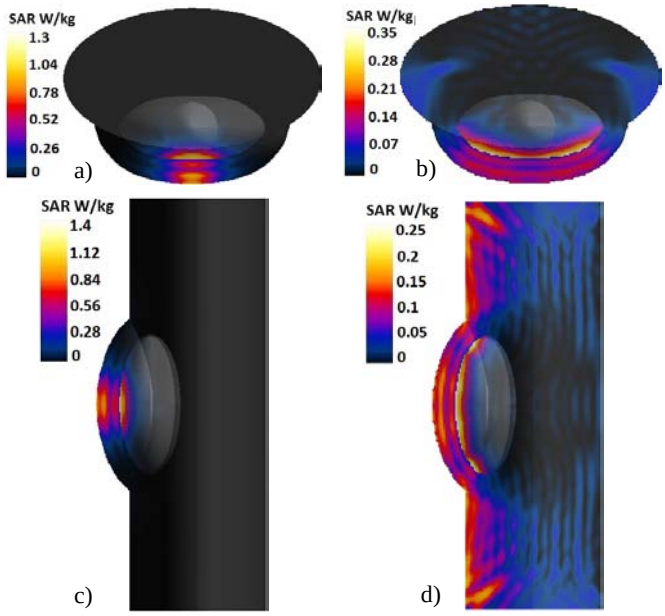

Fig. 14. SAR distribution at 1800 MHz (SEMCAD X):
a) xy plane, dipole source; b) xy plane, plane wave source;
c) yz plane, dipole source; d) yz plane, plane wave source

REFERENCES

[1] J. W. Hand, "Modeling the interaction of electromagnetic fields (10 MHz–10 GHz) with the human body: methods and applications," *Physics in Medicine and Biology*, vol. 53, no. 16, p.p. 243-286, August 2008.
[2] K. Nagasawa, H. Kawai, M. Takahashi, K. Saito, K. Ito, T. Ueda, M. Saito, H. Ito, H. Osada, Y. Koyanagi and K. Ogawa, "Experimental evaluation of the EM exposure in the simple abdomen solid phantom," *Proceedings of ISAP2005*, Seul, Korea, p.p. 881-884, August 2005.
[3] Y. Koyanagi, H. Kawai, K. Ogawa, H. Yoshimura and K. Ito, "Estimation of the radiation and SAR characteristics of the NHA at 150 MHz by use of the cylindroid whole body phantom," *International Symposium on Antennas and Propagation*, Boston, USA, vol. 3, p.p. 78-81, July 2001.
[4] K. Ito and H. Kawai, "Phantoms for evaluation of interactions between antennas and human body," *International Symposium on Electromagnetic Theory – URSI EMT-S 2004*, Pisa, Italy, vol. 2, p.p. 1104-1106, May 2004.
[5] T. Nagaoka, K. Saito, M. Takahashi, K. Ito and S. Watanabe, "Estimating specific absorption rates in pregnant women by using models at 12-, 20- and 26-weeks' gestation for plane wave exposures," *International Symposium on Electromagnetic Compatibility – EMC Europe*, Hamburg, Germany, p.p. 1-4, September 2008.
[6] B. Kos, A. Zupanic, B. Valic, T. Kotnik and P. Gajsek, "Exposure of mother and fetus to electromagnetic fields," *6th International Workshop on Biological Effects of Electromagnetic Fields*, Bodrum, Turkey, p.p. 1-5, October 2010.
[7] T. Togashi, T. Nagaoka, K. Saito, M. Takahashi, K. Ito, S. Watanabe, T. Ueda, M. Saito, H. Ito and H. Osada, "Development of Japanese 7-month pregnant woman model and evaluation of SAR generated by mobile radio terminals," *1st European Conference on Antennas and Propagation – EuCAP 2006*, Nice, Italy, p.p. 1-4, August 2006.
[8] A. Hirata, S. Matsuyama and T. Shiozawa, "Temperature rises in the human eye exposed to EM waves in the frequency range 0.6-6 GHz," *IEEE Transactions on Electromagnetic Compatibility*, vol. 42, no. 4, p.p. 386-393, November 2000.
[9] A. Hirata, "Temperature increase in human eyes due to near-field and far-field exposures at 900 MHz, 1.5 GHz, and 1.9 GHz," *IEEE Transactions on Electromagnetic Compatibility*, vol. 47, no. 1, p.p. 68-76, February 2005.
[10] J. W. Hand, Y. Li and J. V. Hajnal, "Numerical study of RF exposure and the resulting temperature rise in the foetus during a magnetic resonance procedure," *Physics in Medicine and Biology*, vol. 55, no. 8, p.p. 913-930, January 2010.
[11] H. Kawai, Y. Koyanagi, K. Ogawa, K. Sato and K. Ito, "A study on the evaluation of the electromagnetic exposure in the human fetus model at 150 MHz," *Antennas and Propagation Society International Symposium*, vol. 3, p.p. 1087-1090, June 2003.
[12] *ICNIRP: Guidelines for limiting exposure to time-varying electric, magnetic, and electromagnetic fields (up to 300 GHz)*, Healt Phys., vol. 74, p.p. 494-522, 1998.
[13] Z. Živković, D. Despalatović, D. Poljak, A. Šarolić and K. El Khamlici Drissi, "Assessment of SAR Distribution in the Human Eye and Pregnant Woman Models Exposed to RF Radiation Using FEKO Software Package," *19th International Conference on Software, Telecommunications & Computer Networks – SoftCom 2011*, Hvar, Croatia, p.p. 1-5, September 2011.
[14] FEKO - EM simulation software, www.feko.info
[15] SEMCAD X by SPEAG, www.speag.com
[16] H. Dodig, *EM and Thermal Modeling of the Human Eye*, Master's thesis, Wessex Institute of Technology, 2004.
[17] *Dielectric properties of body tissues*, http://niremf.ifac.cnr.it/tissprop/
[18] A. Peratta, "3D low frequency electromagnetic modeling of the human eye with boundary elements: Application to conductive keratoplasty," *Engineering Analysis with Boundary Elements*, vol. 32, no. 8, p.p. 726-735, September 2008.
[19] A. W. Guy, C. Chou and B. Neuhaus, "Average SAR and SAR distributions in man exposed to 450-MHz radiofrequency radiation," *IEEE Transactions on Microwave Theory and Techniques*, vol. 32, no. 8, p.p. 752-763, August 1984.

Zlatko Živković received the Diploma Engineer degree in Electrical Engineering in 2007 from the Faculty of Electrical Engineering, Mechanical Engineering and Naval Architecture, University of Split, Croatia.
He is currently a research assistant and PhD student at the University of Split, Faculty of Electrical Engineering, Mechanical Engineering and Naval Architecture (FESB), Department of Electronics. His research interests are: electromagnetic measurements, bioeffects of EM fields, electromagnetic compatibility (EMC) and radiocommunications.

Duje Despalatović received the M.Sc.E.E. degree in Electrical Engineering in 2010 from the Faculty of Electrical Engineering, Mechanical Engineering and Naval Architecture, University of Split, Croatia. He contributed this paper through his graduation thesis.

Dragan Poljak (M'96) was born in Split, Croatia, in 1965. He received the B.Sc. degree in 1990, the M.Sc. degree in 1994, and the Ph.D. degree in Electrical Engineering in 1996, all from the University of Split, Split.
He is currently a full-time Professor in the Department of Electronics, University of Split, and he is also an Adjunct Professor at the Wessex Institute of Technology, Southampton, Hampshire, U.K. His research interests include frequency and time-domain computational methods in electromagnetics, particularly in the numerical modeling of wire antenna structures, and recently numerical modeling applied to environmental aspects of electromagnetic fields. He has published more than 200 journal and conference papers in the area of computational electromagnetics, seven authored books and one edited book, by WIT Press, Southampton-Boston, MA, and one book by Wiley, Hoboken, NJ.
Dr. Poljak is a member of the editorial board of the journal *Engineering Analysis with Boundary Elements*, and Cochairman of the WIT International Conference on Computational Methods in Electrical Engineering and Electromagnetics. He is also the editor of the WIT Press Series *Advances in Electrical Engineering and Electromagnetics*. Recently, he has been awarded by the *National Prize for Science*.

Antonio Šarolić received the Diploma Engineer, MS and PhD degrees in Electrical Engineering in 1995, 2000 and 2004 from the University of Zagreb, Croatia. He was employed at the same university from 1995 to 2005, at the Faculty of Electrical Engineering and Computing (FER), Dept. of Radiocommunications. In 2006 he joined the University of Split, FESB, Department of Electronics and is now Associate Professor in Electrical Engineering. His areas of interest are electromagnetic measurements, bioeffects of EM fields, electromagnetic compatibility (EMC) and radiocommunications.

Khalil El Khamlichi Drissi is actually Professor and head of the Electrical Engineering department at Polytech'Clermont Ferrand at the Blaise Pascal University. As researcher at LASMEA Laboratory, his research interests include EMC in Power Electronics and Power Systems, especially numerical modeling, EMI reduction and converter control.

He is member of different scientific societies and President of the SEE Auvergne since 1 July 2002 (Society of Electricity, Communication, Electronics and Information Technologies) and Senior Member from December 2, 2003. He is author or coauthor of more than 100 scientific papers published in reviewed journals and presented at international conferences. Prof. El Khamlichi Drissi is a member of IEEE and EEA and has been chairperson and member of scientific committees at international conferences.

Prof. El Khamlichi Drissi is project leader and responsible for several international projects related to EMC (FP7 Marie Curie, Integrafm, Cedre, etc…) and a partner within the Brain City Research Institute. He is actually collaborating with different companies (IFP, EDF, France Telecom and Landis+Gyr).